Peer-reviewed version available at Polymers 2018, 10, 1259; doi:10.3390/polym10111259

Novel Multifunctional Luminescent Electrospun Fluorescent Nanofiber Chemosensors-filter and Their Versatile Sensing of pH, Temperature, and Metal Ions

Bo-Yu Chen [1,2,+], Yen-Chen Lung [2,+], Chi-Ching Kuo [2,3,*], Fang-Cheng Liang [2], Tien-Liang Tsai [2], Dai-Hua Jiang [2], Toshifumi Satoh [4], Ru-Jong Jeng [1,5,*]

[1] Institute of Polymer Science and Engineering, National Taiwan University, 106 Taipei, Taiwan; leodapon@gmail.com (B.-Y.C.); rujong@ntu.edu.tw (R.-J.J.)

[2] Institute of Organic and Polymeric Materials, National Taipei University of Technology, 10608 Taipei, Taiwan; iduo1125@hotmail.com (Y.-C.L.); kuocc@mail.ntut.edu.tw (C.-C.K.); frank62112003@yahoo.com.tw (F.-C.L.); x1x2x310@gmail.com (T.-L.T.); asdf8289@yahoo.com.tw (D.-H.J.)

[3] Research and Development Center for Smart Textile Technology, National Taipei University of Technology, 10608 Taipei, Taiwan; kuocc@mail.ntut.edu.tw (C.-C.K.)

[4] Graduate School of Chemical Sciences and Engineering and Faculty of Engineering, Hokkaido University, Sapporo 060-8628, Japan; satoh@eng.hokudai.ac.jp (T.S.)

[5] Advanced Research Center of Green Materials Science and Technology, National

Taiwan University, 106 Taipei, Taiwan; rujong@ntu.edu.tw (R.-J.J.)

+ Bo-Yu Chen and Yen-Chen Lung contributed equally to this work

*Author to whom all correspondence should be addressed

- kuocc@mail.ntut.edu.tw; Tel.: 886-2-27712171 (ext. 2407); Fax: 886-2-27317174
- Correspondence: Prof. Chi-Ching Kuo (E-mail: kuocc@mail.ntut.edu.tw)

Prof. Ru-Jong Jeng (E-mail: rujong@ntu.edu.tw)

Peer-reviewed version available at *Polymers* **2018**, *10*, 1259; doi:10.3390/polym10111259

Abstract: Novel multifunctional fluorescent chemosensors composed of electrospun (ES) nanofibers with high sensitivity toward pH, mercury ions (Hg^{2+}), and temperature were prepared from poly(*N*-Isopropylacrylamide-*co*-*N*-methylolacrylamide-*co*-rhodamine derivative) (poly(NIPAAm-*co*-NMA-*co*-RhBN2AM)) by employing electrospinning process. NIPAAm and NMA moieties provide hydrophilic and thermo-responsive properties (absorption of Hg^{2+} in aqueous solutions), and chemical cross-linking sites (stabilization of the fibrous structure in aqueous solutions), respectively. The fluorescent probe, RhBN2AM is highly sensitive toward pH and Hg^{2+}. Synthesis of poly(NIPAAm-*co*-NMA-*co*-RhBN2AM) with different compositions were carried on via free-radical polymerization. ES nanofibers prepared from sensory copolymers with a 71.1:28.4:0.5 NIPAAm: NMA: RhBN2AM ratio (**P3** ES nanofibers) exhibited significant color change from nonfluorescent to red fluorescence while sensing pH or Hg^{2+}, and high reversibility of on/off switchable fluorescence emission when Hg^{2+} and ethylenediaminetetraacetic acid (EDTA) were sequentially added. The **P3** ES nanofibrous membranes had a higher surface-to-volume ratio to enhance their performance than did the corresponding thin films. In addition, the fluorescence emission of **P3** ES nanofibrous membranes exhibited second enhancement above the lower critical solution temperature. Thus, the ES nanofibrous membranes prepared from **P3** with on/off switchable

Peer-reviewed version available at Polymers 2018, 10, 1259; doi:10.3390/polym10111259

capacity and thermo-responsive characteristics can be used as multifunctional sensory devise for specific heavy transition metal (HTM) in aqueous solutions.

Keywords: electrospun nanofibers; pH; mercury ion; chemosensor; thermo-response

1. Introduction

Some studies have demonstrated the adverse effects of exposure to heavy transition metal (HTM) cations on children's health, such as low birth weight, low anogenital distance, and severe DNA and chromosome damage. Exposure to methylmercury can lead to Minamata disease, the typical symptoms of which are sensory disturbances (glove and stocking type), ataxia, dysarthria, constriction of the visual field, auditory disturbances, and tremors in some cases [1-3]. Therefore, selective and sensitive chromogenic or fluorogenic chemosensors for various HTM cations detection [4-8] have been designed to solve the aforementioned issues. Kaewtong et al. investigated fluorescent chemosensors composed of a rhodamine-based scaffold and pseudo azacrown cation-binding subunit. The chemosensors exhibited on/off fluorescence emission toward mercury ion (Hg^{2+}) chelation in an organic solution with a short response time, low background interference, low detection limits, long wavelength emission,

Peer-reviewed version available at Polymers 2018, 10, 1259; doi:10.3390/polym10111259

and high selectivity [7]. Recent studies have demonstrated the high potential of rhodamine B (RhB)-copolymer-based chemosensors for temperature, pH, and certain HTM cations sensing in aqueous solutions because of their water solubility, simplicity, ability to change color, and high selectivity [9-15]. Liu et al. reported multifunctional fluorescent copolymers containing RhB moieties that could be used as ultrasensitive fluorometric chemosensors in aqueous media. Their multicolor emission can be effectively tuned by adjusting the temperature, pH [11,13], Zn^{2+} concentration [15], and Hg^{2+} concentration [9,10,12]. However, the primary concern with solution-based chemosensors is that they are not reusable. Wu et al. reported a reusable polymer film chemosensor prepared from a surface modified with a polyvinyl alcohol film probe that can mitigate this defect [16]. However, the aforementioned studies have all used solutions [9-15] or polymeric films [16,17] rather than ES nanofibers. Nanofibers with a high surface-to-volume ratio are expected to enhance responses for temperature, Hg^{2+}, and pH sensing, and also provide reversibility.

The electrospinning process is inexpensive, facile, and versatile for producing sub-micron scale fibers, which has been used extensively in many studies and applications [18-27]. Various florescent electrospun (ES) polymer nanofiber-based chemosensors in our previous studies were designed for sensing pH [28-32], temperature [33-35], and NO gas [36].

Notably, some studies have reported fluorescent ES nanofiber-based chemosensors for sensing specific HTMs such as Fe^{3+} [29], Hg^{2+} [28,31,32,35,37], Zn^{2+} [30,37], and Cu^{2+} [31,37]. We previously reported a novel fluorescent chemosensory ES nanofibrous membrane with high selectivity and reversibility toward pH- and Hg^{2+}, which was prepared using poly(hydroxyethyl-*co*-*N*-methylolacrylamide-*co*-rhodamine derivative) copolymers. In addition, the high surface-to-volume ratio for ES nanofibers affords them with higher sensitivity relative to that of thin films [28]. Moreover, ES nanofibers with thermo-responsive properties have attracted considerable attention because their morphology and diameter can be effectively tuned using environmental temperature, and thus they can be used in many applications such as new types of chemosensors and drug carriers [38-40]. Chiu et al. reported that cross-linked poly(*N*-Isopropylacrylamide-*co*-NMA) (poly(NIPAAm-*co*-NMA)) copolymer-based ES nanofibers could maintain their shape when immersed in water, during which time they exhibited different swelling performance, lower critical solution temperature (LCST), and morphology at various temperatures [39,40]. In the present study, we attempted to put together the aforementioned advantages to develop multifunctional ES fibrous chemosensors capable of temperature-, pH-, and Hg^{2+}-sensing. The chemosensors prepared from sensory copolymers with different NMA ratios for cross-linking reactions exhibited

Peer-reviewed version available at Polymers 2018, 10, 1259; doi:10.3390/polym10111259

different morphologies, LCSTs, and degrees of swelling when immersed in water. Most notably, the chemosensor can be used as multifunctional device for pH-sensing and specific HTMs-chelating, and the intensity of fluorescence emission can be modulated by temperature tuning.

In this study, we report chromo- and fluorogenic sensory nanofibrous membranes prepared using poly(N-isopropylacrylamide-*co*-*N*-methylolacrylamide-*co*-rhodamine derivative) (poly(NIPAAm-*co*-NMA-*co*-RhBN2AM)) copolymers. Due to the presence of a hydrophilic and thermo-responsive moiety (PNIPAAm), a chemical cross-linkable moiety (PNMA), and a fluorescent probe with Hg^{2+}-chelating and pH-sensing characteristics (RhBN2AM), the sensory nanofibrous membranes exhibited multifunctional sensory characteristics for Hg^{2+}, pH, and temperature sensing. The nanofibrous membranes were prepared from poly(NIPAAm-*co*-NMA-*co*-RhBN2AM), which was synthesized through free-radical polymerization. The polymerization schematic and the sensing mechanism of RhBN2AM are shown in Scheme 1(a). Their LCSTs, optical properties, and morphological characteristics were analyzed. The electrospinning process was used to fabricate ES nanofibers from poly(NIPAAm-*co*-NMA-*co*-RhBN2AM) (Scheme 1(b)), and the stability enhancement of nanofibers in water was achieved through chemical cross-linking reactions.

Peer-reviewed version available at Polymers 2018, 10, 1259; doi:10.3390/polym10111259

In addition, Scheme 1(c) shows that the sensory ES nanofibers exhibited reversible thermo-induced second fluorescence intensity enhancement when the sample was heated above LCST and subsequently cooled down. The fluorescence emission of RhBN2AM is highly sensitive toward Hg^{2+} or pH. In detection of Hg^{2+} or acidic media, RhBN2AM transformed from its spirocyclic form (colorless and nonfluorescent) into its opened cyclic form (pink and strong fluorescence emission) [7,28]. Thus, the off/on switching of the fluorescence can be facilely modulated by tuning pH levels or Hg^{2+} concentration, meanwhile the fluorescence intensity can be easily tuned through heating or cooling. We further compared the fluorescence emissions of chemosensors prepared from thin films and ES nanofibrous membranes. The favorable reversible property of Hg^{2+}- or pH-sensing indicates that sensory nanofibrous membranes certainly possess the potential for applications in multisensory devices and HTMs filtration.

2. Experimental Section

2.1. Materials

N-Isopropylacrylamide (NIPAAm), *N*-methylolacrylamide (NMA), 2,2'-azobis(2-methylpropionitrile) (AIBN), were purchased from Sigma-Aldrich, Tokyo Chemical Industry Co., and UniRegion Bio-Tech, respectively. They were re-crystallized and stored at 4 °C prior to use. Trizma® baes (Sigma, 99.9%), Rhodamine base (RhB, Sigma-Aldrich, 97%), anhydrous magnesium sulfate ($MgSO_4$, J. T. Baker, assay), Ethylenediamine (Sigma-Aldrich, 99%), acryloyl chloride (Sigma-Aldrich, 97%), triethylamine (TEA, Sigma-Aldrich, 99.5%) were used as received. Methanol (Tedia, HPLC/SPECTRO), ethanol (Sigma-Aldrich, absolute), acetonitrile anhydrous (Tedia, 99%), tetrahydrofuran (THF, Tedia, HPLC), and dichloromethane (Tedia, 99.9%) were used as received. All perchlorate salts of metal ions were obtained from Aldrich.

2.2. Characterization

^{1}H nuclear magnetic resonance (NMR) data was recorded at room temperature on a Bruker AM 300 (300MHz) spectrometer using the residual proton resonance of the deuterated chloroform and deuterated dimethyl sulfoxide. The LCST (phase transition) of the prepared copolymer solution was recorded by monitoring the transmittance of a 540 nm light beam on

Shimadzu UV–Vis spectrophotometer. The copolymer concentration in water was 1 wt%, and the temperature was raised from 25 to 70 °C in 2.5 °C increment for every 10 min [35,36]. Thermal analysis was carried out via a thermogravimetric analyzer (TGA) from TA instrument (TA Q500) with a heating range from 100 to 700 ℃ at a heating rate of 10 ℃ min^{-1}. The morphologies of ES nanofibers were investigated through Field Emission Scanning Electron Microscope (SEM, FEI Inspect S) and a two-photon laser confocal microscope (Leica LCS SP5). Photoluminescence (PL) spectra were measured to study photophysical properties, which were recorded using a Fluorolog-3 spectrofluorometer (Horiba Jobin Yvon). All PL spectra of ES Nanofiber for pH and Hg^{2+} sensing were recorded using the Fluorolog-3 spectrofluorometer and excited at a wavelength of 540 nm, as described in Supporting Information, which is similar to that in our previous studies [28-37].

2.3. Synthesis of the fluorescent probe (RhBN2) and fluorescent monomer (RhBN2AM)

The synthetic scheme for *RhBN2AM* is shown in Scheme 2(a). The syntheses of fluorescent probes, RhBN2 and RhBN2AM, were performed according to literature [7,28]. The detailed procedures are shown in Supporting Information. The chemical structure of RhBN2AM was characterized using ^1H NMR (**Figure S1(a)**) and ESI-MS (**Figure S1(b)**)

2.4. Synthesis of poly(NIPAAm-co-NMA-co-RhBN2AM)

The synthetic scheme for poly(NIPAAm-co-NMA-co-RhBN2AM) is shown in Scheme 2(b). Poly(NIPAAm-*co*-NMA-*co*-RhBN2AM) copolymers with different NMA ratios were denoted **P1**, **P2**, and **P3**, as listed in Table 1. In a round bottomed two-necked flask, NIPAAm (1.59 g, 14.1 mmol), NMA (712.1 mg, 7.05 mmol), RhBN2AM (75.6 mg, 0.14 mmol), AIBN (4.3mg, 0.026 mmol) were dissolved in ethanol. Nitrogen bubbling was maintained for 30 min to remove oxygen. Subsequently, the mixture was immersed in oil bath at 70 °C for 24 h. The polymerization was quenched by exposure to air. In order to remove unreacted monomers, the solution was diluted with ethanol, precipitated in ether, and then freeze-dried until constant weight, the polymer **P3** was obtained. Characterization of **P3** by GPC and ^{1}H NMR are shown in **Figure S2** and **Figure S3**, respectively. The copolymer composition of **P3** based on the NMR spectrum is estimated to be 71.1:28.4:0.5. Number-averaged molecular weight (M_n) = 35500 g mol^{-1}, and polydispersity index (M_w/M_n) = 1.88 were obtained from GPC measurement using DMF as an eluent (**Figure S3**). ^{1}H NMR (300 MHz, DMSO, δ, ppm; **Figure S2**): 8.08 (h), 7.25 (g), 5.46 (f), 4.43 (e), 3.79 (d), 1.88 (c), 1.43 (b), 0.93 (a).

2.5. Preparation of electrospun fibers and drop-cast films

The ES nanofibers were fabricated using electrospinning process as described in Scheme

Peer-reviewed version available at Polymers 2018, 10, 1259; doi:10.3390/polym10111259

1(b), similar to that in our previous reports [28-37]. The polymer solution of **P1**, **P2**, and **P3,** (400 mg mL^{-1} dissolved in a methanol (MeOH)) were filled into a metallic needle by using syringe pumps (KD Scientific Model 100, USA), and a feed rate at 1 mL h^{-1}. A high-voltage power supply (Chargemaster CH30P SIMCO, USA) was set at 10 kV during the ES process. On the other hand, the corresponding films of **P1**, **P2**, and **P3** were respectively drop-cast on glass substrates using the same concentration and volume of the polymer solution. For chemical cross-linking, all samples were treated at 120 °C for 48 h in an oven, which was similar to that reported in our previous studies [28,29,31,35-37].

3. Results and Discussion

3.1. Characterization of RhBN2AM, and poly(NIPAAm-co-NMA-co-RhBN2AM)

The chemical structure of RhBN2AM was characterized using ^{1}H NMR (**Figure S1(a)**) and ESI-MS (**Figure S1(b)**). The synthetic routes of RhBN2AM are shown in Scheme 2(a) which are similar to that in previous studies [7,28]. Poly(NIPAAm-*co*-NMA-*co*-RhBN2AM) copolymers with three different molar ratios of NMA, denoted as **P1**, **P2**, and **P3,** were synthesized via free-radical polymerization according to Scheme 2(b). **Figure S2** shows the ^{1}H NMR spectra of poly(NIPAAm-*co*-NMA-*co*-RhBN2AM) copolymers, which were

composed of NIPAAm, NMA, and RhBN2AM in ratios of 90.2:9.4:0.4 (**P1**), 80.5:19.2:0.3 (**P2**), and 71.1:28.4:0.5 (**P3**) in DMSO. The proton peak for DMSO is shown in **Figure S2**. The proton peaks at 3.79 ppm (peak d) represent the methine neighbor of the methyl group on NIPAAm. The peaks at 8.08 (peak h) and 5.46 (peak f) ppm represent the secondary amine moiety and terminal hydroxyl moiety of NMA, respectively. Peak integrations for peaks g, h, and f increased with increasing NMA content. The peak at 0.93 ppm (peak a) represents the alkyl chains on the polymer. The copolymer composition estimated by performing peak integration was consistent with the proposed structure. The $M_{n,\,GPC\,(DMF)}$ and M_w/M_n of the **P1**, **P2**, and **P3** copolymers were 33 000 and 1.85, 35 300 and 1.92, and 35 500 and 1.88, respectively, as shown in Table 1 and **Figure S3**. The LCSTs of the **P1**, **P2**, and **P3** copolymers were 30.0, 35.0, and 45.0 °C, respectively, as shown in Table 1 and **Figure S4**. The thermal decomposition thermograms of the prepared copolymers are shown in **Figure S5**. The thermal decomposition temperatures (T_d) of **P1**, **P2**, and **P3** were 343, 351, and 352 °C, as shown in Table 1, which exhibited favorable and stable thermal properties.

3.2. Morphologies of Electrospun Nanofibers

Figure 1 (a) shows the field emission scanning electron microscopy images of the as-

Peer-reviewed version available at Polymers 2018, 10, 1259; doi:10.3390/polym10111259

spun ES nanofibers prepared from poly(NIPAAm-*co*-NMA-*co*-RhBN2AM) copolymers (**P1**, **P2**, and **P3**) in dry and wet states. These ES nanofibers were cross-linked through thermo-treating the samples at 120 °C for 48 h. The diameter ranges of the **P1**, **P2**, and **P3** ES nanofibers were estimated as 513 ± 28, 475 ± 35, and 412 ± 44 nm, respectively. The average diameter value was based on the statistical average of 50 fibers from each sample. Similar fiber diameters are a result of comparable polymer molecular weights, all approximately Mn = 35 000 (Table 1) and the use of similar ES process parameters.

To observe the morphology of the cross-linked **P1**, **P2**, and **P3** ES nanofibers after Hg^{2+} or H^{+} sensing in an aqueous solution, the nanofibers were collected on a small piece of aluminum foil and immersed in water with Hg^{2+} or placed under an acidic condition. After detection, the samples were dried by freeze-drying for 30 min to remove the residual water to retain the original morphology. **Figure 1 (a)** shows SEM images of the **P1**, **P2**, and **P3** ES nanofibers in the wet state after 10^{-3} M Hg^{2+} sensing. To compare with the irregular films that derived from the **P1** and **P2** ES nanofibers, the **P3** ES nanofibers maintained a cylindrical shape after being extracted from the aqueous solution, as shown in **Figure 1 (a)** (wet state, 20 °C), and exhibited fiber diameters of approximately 1 μm. The results indicate that **P1** was mostly soluble and **P2** was slightly soluble in water because of the insufficient NMA content

Peer-reviewed version available at Polymers 2018, 10, 1259; doi:10.3390/polym10111259

for cross-linking to maintain the fiber morphologies. These swollen fibers maintained their cylindrical shape and did not dissolve in water because of the efficient chemical cross-linking of the NMA moieties, a result similar to that of our previous studies [28,29,31,35,37]. However, the fiber diameters of the **P2** and **P3** ES nanofibers shrank significantly (approximately 2.5-fold, from 1000 to 400 nm) after the nanofibers were heated in water (wet state, 60 °C; temperature above LCST) because the PNIPAAm chain (thermo-responsive) disintegrated in water, as shown in **Figure 1 (a)** (wet state, 60 °C) and **Figure 1 (b)**. The fiber diameters would vary as the temperature changed. In fact, the diameter decreased while temperature increased from 20 to 60 °C, effectively enhancing the sensitivity of the fluorogenic chemosensors, as demonstrated by PL spectra.

3.3. pH sensing property of ES Nanofibers

Figure 2(a) presents the PL spectra of **P2-fibers** in an aqueous solution with various pH levels (pH 7–2) at room temperature. The PL intensity of emission maxima ($\lambda_{PL,\ max}$) at 584 nm gradually increased as the pH value decreased (from pH 7 to 2). When RhBN2AM detected H^+, the RhBN2AM transformed from its non-fluorescent spirocyclic form into its opened cyclic form, a strong fluorescence, with $\lambda_{PL,\ max}$ at 584 nm. As the inset of the figure

shows, the PL intensity was quenched at pH 12, indicating that the poly(NIPAAm-*co*-NMA-*co*-RhBN2AM) copolymers were pH-dependent. In **Figure 2(b)**, the tendency of **P3-fibers** is identical to that shown in **Figure 2(a)**. In the inset of **Figure 2(b)**, **P3-fibers** exhibited off/on switchable fluorescence emission at pH 12 and 2. However, the $\lambda_{PL,\ max}$ of **P3-fibers** was higher than that of **P2-fibers** because the cross-linked **P3-fibers** possessed a higher content of NMA. This would enable them to maintain their cylindrical shape, and a higher surface-to-volume ratio. The results indicate that **P3-fibers** were more sensitive toward pH changes than **P2-fibers**. **Figure 2(c)** presents the thermo-dependent characteristics of **P2-fibers** at a constant pH level (pH 2). As the temperature increased from 27 to 55 °C, the PL intensity of the $\lambda_{PL,\ max}$ at 584 nm increased (approximately 3.4-fold) for **P2-fibers** due to the disintegration of the thermoresponsive polymer chains (PNIPAAm) (55 °C; temperature above LCST). This is because the probe to probe (RhBN2AM to RhBN2AM) distance within the copolymer chains became narrower. The aggregation of probes led to enhancement of the $\lambda_{PL,\ max}$, and the results are similar to those reported in previous studies [12,15,34]. Despite of similar thermo-dependent characteristics to those of **P2-fibers** (**Figure 2(d)**), the $\lambda_{PL,\ max}$ of **P3-fibers** exhibited a 4.8-fold enhancement indicating that **P3-fibers** were more dependent on pH and temperature than **P2-fibers**.

Peer-reviewed version available at Polymers 2018, 10, 1259; doi:10.3390/polym10111259

3.4. Hg^{2+} sensing property of ES Nanofibers

RhBN2AM is a favorable fluorescent probe for sensing pH and Hg^{2+}. **P3-fibers** maintained their highly fibrous shape, which enabled excellent sensitivity. Thus, the capability of **P3-fibers** for sensing Hg^{2+} was explored. **Figure 3(a)** shows the PL spectra of **P3-fibers** at different Hg^{2+} concentrations. As the Hg^{2+} concentration increased, the $\lambda_{PL,\ max}$ at 584 nm of **P3-fibers** gradually increased from 10^{-7} to 10^{-3} M because more Hg^{2+} ions were chelated by the RhBN2AM within the ES nanofibers, and the RhBN2AM transformed from its non-fluorescent spirocyclic form into its strongly fluorescent opened cyclic form, with $\lambda_{PL,\ max}$ at 584 nm. In **Figure 3(b)**, **P3-film** exhibited similar fluorescent behavior to that of **P3-fibers**. Nevertheless, **Figure 3(c)** shows that **P3-fibers** exhibited excellent capacity for Hg^{2+} sensing as compared with **P3-film**. This is because the surface-to-volume ratio of **P3-fibers** was higher than that of **P3-film**. These results are similar to those of our previous study [28].

Figure 4(a) shows the PL intensity variation of **P3-fibers** with temperature at a constant Hg^{2+} concentration (10^{-3} M). The $\lambda_{PL,\ max}$ at 584 nm of **P3-fibers** gradually increased (approximately 4.7-fold) when the temperature increased from 27 to 55 °C. **Figure 4(b)** shows the plot of intensity as a function of temperature for **P3-fibers**. Thermo-induced second

Peer-reviewed version available at Polymers 2018, 10, 1259; doi:10.3390/polym10111259

fluorescence intensity enhancement was achieved at temperatures above the LCST (45 °C) because the area of the **P3-fibers** membrane decreased from 1.0 × 0.7 cm (specific size) to 0.8 × 0.5 cm, as shown in the figure inset, thereby exhibiting significant fluorescence emission after Hg^{2+} sensing under an ultraviolet (UV) lamp. The thermo-induced second fluorescence intensity enhancement was possibly due to the reduced fiber diameter, resulting in aggregated and dense Rh-chelated Hg^{2+} moieties.

Figure 5(a) shows the PL spectra recorded in the presence of Hg^{2+} or coexistence with other competing metal ions (Fe^{2+}, Pb^{2+}, Mg^{2+}, Zn^{2+}, Cu^{2+}, and K^{+}) in an aqueous solution. The black bars denote that the presence of Hg^{2+} induced the most significant PL intensity enhancement (approximately 31.7-fold) at 584 nm ($\lambda_{PL,\,max}$), leading to red emission. The red bars denote that the PL spectra recorded in the coexistence of Hg^{2+} ions and other competing metal ions, revealing virtual unaffectedness for Hg^{2+} sensing. This indicates that **P3-fibers** are highly selective toward Hg^{2+} with almost no interference by these commonly coexistence of HTMs in environment. **Figure 5(b)** shows that the fluorescence emission ($\lambda_{PL,\,max}$ at 584 nm) of **P3-fibers** was observably enhanced after the completion of Hg^{2+}-sensing. The fluorescence emission almost completely quenched by adding EDTA. Moreover, the on/off switchable fluorescence emission of **P3-fibers** in aqueous media that occurred upon the sequential

Peer-reviewed version available at Polymers 2018, 10, 1259; doi:10.3390/polym10111259

addition of 10^{-3} M Hg^{2+} and EDTA could be repeated for at least five times. The spirocyclic form of RhBN2AM can be effectively induced to its opened cyclic form through binding with Hg^{2+} ions; this conversion was responsible for the on/off switchable fluorescence emission in this study (the insets show the fluorescence emission variation of the **P3-fibers** membrane recorded under a UV lamp).

3.5. Thermo-responsive volume and luminescence variation of ES nanofibers

P3-fibers exhibited an on/off switchable fluorescence emission in the confocal microscopy images as shown in **Figure 6(a)**. The strong and switchable fluorescence emission was due to the chelation of Hg^{2+} or protonation of H^{+} by RhBN2AM (all inset images were recorded under visible light). **Figure 6(b)** shows the on/off fluorescence emission and thermo-induced second fluorescence intensity enhancement of the **P3** ES nanofibrous membrane (1.0 × 0.7 cm) recorded under a UV lamp. Although the **P3** ES nanofibrous membrane was nonfluorescent in its original state (blank), red fluorescence emission could easily be activated by adding an acidic or Hg^{2+} aqueous solution. However, as shown in **Figure 6(b)**, the area of the ES fibrous membrane changed from 1.0 × 0.7 to 0.8 × 0.5 cm as the temperature increased from 25 to 60 °C. This indicates that the ES fibrous membrane exhibited a rapid and significant shrinkage by 57% of its initial area within 5 min. In addition, the PL intensity of the shrunk

Peer-reviewed version available at Polymers 2018, 10, 1259; doi:10.3390/polym10111259

state at 60 °C was stronger than that of the swollen state at 25 °C under UV light illumination, as shown in images of **Figure 6(b)** and in **Figure 4(b)**, respectively. The thermo-induced second fluorescence intensity enhancement was possibly due to the reduced fiber diameter, which resulted in aggregated and dense Rh-chelated Hg^{2+} moieties. **Figure 7** presents the schematic for preparing the sensory fibrous membranes (1 × 0.7 cm) with a porous architecture based on **P3** sensory copolymers with the intention to apply in filtration of industrial wastewater containing specific HTMs, as well as environmental pH and temperature sensing. The robustness of the fibrous membranes with high absorption efficiency in Hg^{2+} filtration is similar to that in our previous research [28], as indicated by the significantly decreased concentration of Hg^{2+} ions in a very short period of time. The **P3**-based ES nanofibrous membranes with a porous architecture and high surface-to-volume ratios possess considerable potential to be applied in water purification because of their effectiveness in absorbing Hg^{2+} in aqueous environment. In addition, the fluorescence emission could be drastically enhanced at temperatures above the LCST. The rapid thermo-induced fluorescence emission or volume variation is due to the high surface-to-volume ratio of the ES nanofibers. Based on the above, the **P3**-based ES nanofibrous membranes have the potential to play the role of multifunctional sensory devices.

Peer-reviewed version available at Polymers 2018, 10, 1259; doi:10.3390/polym10111259

4. Conclusions

Novel multifunctional ES fibrous membranes with on/off switchable fluorescence emission properties, thermo-induced second fluorescence intensity enhancement characteristics, and high sensitivity toward pH and Hg^{2+} were prepared using poly(NIPAAm-*co*-NMA-*co*-RhBN2AM) (**P3**) by electrospinning process. The NIPAAm, NMA, and RhBN2AM moieties in this study were designed to provide hydrophilic and thermo-responsive properties, chemical cross-linking feature, and fluorescent probes, respectively. The **P3** ES nanofibers sufficient NMA content were capable of maintaining their fibrous cylindrical shape when immersed in aqueous solution for pH and Hg^{2+} sensing. The fluorescence emission of the RhBN2AM within the ES nanofibers was highly sensitive toward pH and Hg^{2+} (i.e., non-fluorescence in neutral or alkaline media or an aqueous solution without Hg^{2+} (spirocyclic form); but strong fluorescence in acidic media or aqueous solutions with Hg^{2+} (ring-opened cyclic form)). Thus, the off/on switchable properties of the fluorescence emission can be facilely modulated by tuning the pH and Hg^{2+} concentration. In addition, the degree of disintegration of the **P3** ES nanofibers was dependent on the temperature, resulting in a decrease in the probe–probe (RhBN2AM–RhBN2AM) distance

Peer-reviewed version available at Polymers 2018, 10, 1259; doi:10.3390/polym10111259

and further enhancement of the red fluorescence emission. Substantial reversible PL emission from the **P3** ES nanofibrous membrane was also observed in Hg^{2+} and EDTA aqueous solutions for at least five times. This study demonstrates that the prepared fluorescent ES nanofibrous membranes, which can be used as "naked eye" sensors, have marked advantages for applications in multifunctional devices for specific HTM chelation, as well as pH and temperature sensing in aqueous environments.

Peer-reviewed version available at *Polymers* **2018**, *10*, 1259; doi:10.3390/polym10111259

Supplementary Materials: Figure S1: (a) 1H NMR spectrum of RhBN2AM in CDCl3. (b) ESI-MS spectrum of RhBN2AM. Figure S2: 1H NMR spectra of **P1**, **P2**, and **P3**. Figure S3: GPC profiles of **P1**, **P2**, and **P3**. Figure S4: Variations in optical transmittance of **P1**, **P2**, and **P3** in water at temperatures from 25 to 70 °C. Figure S5: TGA curves of **P1**, **P2**, and **P3**.

Acknowledgment: We acknowledges the Ministry of Science and Technology, Taiwan, and National Taipei University of Technology, (MOST 106-2221-E-027 -119 -MY3 and MOST 107-3017-F-002-001), for financial support.

Author Contributions: Bo-Yu Chen, Yen-Chen Lung, Fang-Cheng Liang, Tien-Liang Tsai, Dai-Hua Jiang and Chi-Ching Kuo conceived and designed the experiments; Bo-Yu Chen, Yen-Chen Lung, Fang-Cheng Liang, Tien-Liang Tsai, Dai-Hua Jiang performed the experiments; Chi-Ching Kuo, Toshifumi Satoh and Ru-Jong Jeng contributed reagents/materials/analysis tools; Bo-Yu Chen, Yen-Chen Lung and Chi-Ching Kuo analyzed the data and complete the paper.

Conflicts of Interest: The authors declare no conflict of interest.

References

1. Day, J.J.; Reed, M.N.; Newland, M.C. Neuromotor Deficits and Mercury Concentrations in Rats Exposed to Methyl Mercury and Fish Oil. *Neurotoxicol. Teratol.* **2005**, *27*, 629-641. [CrossRef]

2. Harada, M. Minamata Disease: Methylmercury Poisoning in Japan Caused by

Environmental Pollution. *Crit. Rev. Toxicol.* **1995**, *25*, 1-24. [CrossRef]

3. Zeng, X.; Xu, X.; Boezen, H.M.; Huo, X. Children with Health Impairments by Heavy Metals in an E-Waste Recycling Area. *Chemosphere* **2016**, *148*, 408-15. [CrossRef]

4. Bag, B.; Pal, A. Rhodamine-based Probes for Metal Ion-induced Chromo-/Fluorogenic Dual Signaling and Their Selectivity Towards Hg(II) ion. *Org. Biomol. Chem.* **2011**, *9*, 4467-80. [CrossRef]

5. Chen, X.; Pradhan, T.; Wang, F.; Kim, J.S.; Yoon, J. Fluorescent Chemosensors Based on Spiroring-opening of Xanthenes and Related Derivatives. *Chem. Rev.* **2012**, *112*, 1910-56. [CrossRef]

6. Huang, J.; Xu, Y.; Qian, X. A Rhodamine-Based Hg^{2+} Sensor with High Selectivity and Sensitivity in Aqueous Solution: a NS_2-containing Receptor. *J. Org. Chem.* **2009**, *74*, 2167-2170. [CrossRef]

7. Kaewtong, C.; Wanno, B.; Uppa, Y.; Morakot, N.; Pulpoka, B.; Tuntulani, T. Facile Synthesis of Rhodamine-based Highly Sensitive and Fast Responsive Colorimetric and Off-On Fluorescent Reversible Chemosensors for Hg^{2+}: Preparation of a Fluorescent Thin Film Sensor. *Dalton Trans.* **2011**, *40*, 12578-83. [CrossRef]

8. Zhang, X.; Shiraishi, Y.; Hira, T. Cu(II)-Selective Green Fluorescence of a Rhodamine−Diacetic Acid Conjugate. *Org. Lett.* **2007**, *9*, 5039-5042. [CrossRef]

9. Hu, J.; Dai, L.; Liu, S. Analyte-Reactive Amphiphilic Thermoresponsive Diblock Copolymer Micelles-Based Multifunctional Ratiometric Fluorescent Chemosensors. *Macromolecules* **2011**, *44*, 4699–4710. [CrossRef]

10. Hu, J.; Wu, T.; Zhang, G.; Liu, S. Highly Selective Fluorescence Sensing of Mercury Ions over a Broad Concentration Range Based on Mixed Polymeric Micelles. *Macromolecules*

2012, *45*, 3939−3947. [CrossRef]

11. Hu, J.; Zhang, X.; Wang, D.; Hu, X.; Liu, T.; Zhang, G.; Liu, S. Ultrasensitive Ratiometric Fluorescent pH and Temperature Probes Constructed from Dye-Labeled Thermoresponsive Double Hydrophilic Block Copolymers. *J. Mater. Chem.* **2011**, *21*, 19030–19038. [CrossRef]

12. Li, C.; Liu, S. Responsive Nanogel-Based Dual Fluorescent Sensors for Temperature and Hg^{2+} Ions with Enhanced Detection Sensitivity. *J. Mater. Chem.* **2010**, *20*, 10716–10723. [CrossRef]

13. Li, C.; Zhang, Y.; Hu, J.; Cheng, J.; Liu, S. Reversible Three-State Switching of Multicolor Fluorescence Emission by Multiple Stimuli Modulated FRET Processes within Thermoresponsive Polymeric Micelles. *Angew. Chem., Int. Ed.* **2010**, *49*, 5120-5124. [CrossRef]

14. Lin, S.T.; Fuchise, K.; Chen, Y.; Sakai, R.; Satoh, T.; Kakuchi, T.; Chen, W.C. Synthesis, Thermomorphic Characteristics, and Fluorescent Properties of Poly[2,7-(9,9-dihexylfluorene)]-*block*-Poly(*N*-isopropylacrylamide)-*block*-Poly(N-hydroxyethylacrylamide) Rod-Coil-Coil Triblock Copolymers. *Soft Matter* **2009**, *5*, 3761–3770. [CrossRef]

15. Liu, T.; Liu, S. Responsive Polymers-Based Dual Fluorescent Chemosensors for Zn^{2+} Ions and Temperatures Working in Purely Aqueous Nedia. *Anal. Chem.* **2011**, *83*, 2775-2785. [CrossRef]

16. Ma, B.; Wu, S.; Zeng, F. Reusable Polymer Film Chemosensor for Ratiometric Fluorescence Sensing in Aqueous Media. *Sens. Actuators, B* **2010**, *145*, 451–456. [CrossRef]

17. Lv, F.; Feng, X.; Tang, H.; Liu, L.; Yang, Q.; Wang, S. Development of Film Sensors

Based on Conjugated Polymers for Copper (II) Ion Detection. *Adv. Funct. Mater.* **2011**, *21*, 845–850. [CrossRef]

18. Chen, J.Y.; Kuo, C.C.; Lai, C.S.; Chen, W.C.; Chen, H.L. Manipulation on the Morphology and Electrical Properties of Aligned Electrospun Nanofibers of Poly(3-hexylthiophene) for Field-Effect Transistor Applications. *Macromolecules* **2011**, *44*, 2883–2892. [CrossRef]

19. Chen, Y.Y.; Kuo, C.C.; Chen, B.Y.; Chiu, P.C.; Tsai, P.C. Multifunctional Polyacrylonitrile-ZnO/Ag Electrospun Nanofiber Membranes with Various ZnO Morphologies for Photocatalytic, UV-Shielding, and Antibacterial Applications. *J. Polym. Sci., Part B: Polym. Phys.* **2015**, *53*, 262–269. [CrossRef]

20. Huang, Y.S.; Kuo, C.C.; Huang, C.C.; Jang, S.C.; Tsen, W.C.; Chuang, F.S.; Chen, B.Y.; Chen, J.J.; Chow, J.D.; Shu, Y.C. Novel Highly Aligned, Double-Layered, Hollow Fibrous Polycarbonate Membranes with a Perfectly Tightly Packed Pentagonal Pore Structure Fabricated Using the Electrospinning Process. *RSC Adv.* **2015**, *5*, 88857–88865. [CrossRef]

21. Huang, Y.S.; Kuo, C.C.; Shu, Y.C.; Jang, S.C.; Tsen, W.C.; Chuang, F.S.; Chen, C.C. Highly Aligned and Single-Layered Hollow Fibrous Membranes Prepared from Polyurethane and Silica Blends Through a Two-Fluid Coaxial Electrospun Process. *Macromol. Chem. Phys.* **2014**, *215*, 879−887. [CrossRef]

22. Kuo, C.C.; Lin, C.H.; Chen, W.C. Morphology and Photophysical Properties of Light-Emitting Electrospun Nanofibers Prepared from Poly(fluorene) Derivative/ PMMA Blends. *Macromolecules* **2007**, *40*, 6959-6966. [CrossRef]

23. Kuo, C.C.; Tung, Y.C.; Chen, W.C. Morphology and pH Sensing Characteristics of New Luminescent Electrospun Fibers Prepared from Poly(phenylquinoline)-*block*-

Polystyrene/Polystyrene Blends. *Macromol. Rapid Commun.* **2010**, *31*, 65-70. [CrossRef]

24. Kuo, C.C.; Tung, Y.C.; Lin, C.H.; Chen, W.C. Novel Luminescent Electrospun Fibers Prepared from Conjugated Rod–Coil Block Copolymer of Poly[2,7-(9,9-dihexylfluorene)]-*block*-Poly(methyl methacrylate). *Macromol. Rapid Commun.* **2008**, *29*, 1711–1715. [CrossRef]

25. Kuo, C.C.; Wang, C.T.; Chen, W.C. Highly-Aligned Electrospun Luminescent Nanofibers Prepared from Polyfluorene/PMMA Blends: Fabrication, Morphology, Photophysical Properties and Sensory Applications. *Macromol. Mater. Eng.* **2008**, *293*, 999–1008. [CrossRef]

26. Tzeng, P.; Kuo, C.C.; Lin, S.T.; Chiu, Y.C.; Chen, W.C. New Thermoresponsive Luminescent Electrospun Nanofibers Prepared from Poly[2,7-(9,9-dihexylfluorene)]-*block*-Poly(*N*-isopropylacrylamide)/PMMA Blends. *Macromol. Chem. Phys.* **2010**, *211*, 1408–1416. [CrossRef]

27. Wang, C.T.; Kuo, C.C.; Chen, H.C.; Chen, W.C. Non-Woven and Aligned Electrospun Multicomponent Luminescent Polymer Nanofibers: Effects of Aggregated Morphology on the Photophysical Properties. *Nanotechnology* **2009**, *20*, 375604. [CrossRef]

28. Chen, B.Y.; Kuo, C.C.; Cho, C.J.; Liang, F.C.; Jeng, R.J. Novel Fluorescent Chemosensory Filter Membranes Composed of Electrospun Nanofibers with Ultra-Selective and Reversible pH and Hg^{2+} Sensing Characteristics. *Dyes Pigm.* **2017**, *143*, 129-142. [CrossRef]

29. Chen, B.Y.; Kuo, C.C.; Huang, Y.S.; Lu, S.T.; Liang, F.C.; Jiang, D.H. Novel Highly Selective and Reversible Chemosensors Based on Dual-Ratiometric Fluorescent Electrospun Nanofibers with pH- and Fe^{3+}-Modulated Multicolor Fluorescence Emission. *ACS Appl.*

Mater. Interfaces **2015**, *7*, 2797-2808. [CrossRef]

30. Chen, L.N.; Kuo, C.C.; Y.C., Chiu; Chen, W.C. Ultra Metal Ions and pH Sensing Characteristics of Thermoresponsive Luminescent Electrospun Nanofibers Prepared from Poly(HPBO-*co*-NIPAAm-*co*-SA). *RSC Adv.* **2014**, *4*, 45345–45353. [CrossRef]

31. Cho, C.J.; Lu, S.T.; Kuo, C.C.; Liang, F.C.; Chen, B.Y.; Chu, C.C. Pyrene or Rhodamine Derivative–Modified Surfaces of Electrospun Nanofibrous Chemosensors for Colorimetric and Fluorescent Determination of Cu^{2+}, Hg^{2+}, and pH. *React. Funct. Polym.* **2016**, *108*, 137-147. [CrossRef]

32. Liang, F.C.; Kuo, C.C.; Chen, B.Y.; Cho, C.J.; Hung, C.C.; Chen, W.C.; Borsali, R. RGB-Switchable Porous Electrospun Nanofiber Chemoprobe-Filter Prepared from Multifunctional Copolymers for Versatile Sensing of pH and Heavy Metals. *ACS Appl. Mater. Interfaces* **2017**, *9*, 16381-16396. [CrossRef]

33. Chiu, Y.C.; Chen, Y.; Kuo, C.C.; Tung, S.H.; Kakuchi, T.; Chen, W.C. Synthesis, Morphology, and Sensory Applications of Multifunctional Rod-Coil-Coil Triblock Copolymers and Their Electrospun Nanofibers. *ACS Appl. Mater. Interfaces* **2012**, *4*, 3387-3395. [CrossRef]

34. Chiu, Y.C.; Kuo, C.C.; Hsu, J.C.; Chen, W.C. Thermoresponsive Luminescent Electrospun Fibers Prepared from Poly(DMAEMA-*co*-SA-*co*-StFl) Multifunctional Random Copolymers. *ACS Appl. Mater. Interfaces* **2010**, *2*, 3340-3347. [CrossRef]

35. Liang, F.C.; Luo, Y.L.; Kuo, C.C.; Chen, B.Y.; Cho, C.J.; Lin, F.J.; Yu, Y.Y.; Borsali, R. Novel Magnet and Thermoresponsive Chemosensory Electrospinning Fluorescent Nanofibers and Their Sensing Capability for Metal Ions. *Polymers* **2017**, *9*, 136. [CrossRef]

36. Chen, L.N.; Chiu, Y.C.; Hung, J.J.; Kuo, C.C.; Chen, W.C. Multifunctional Electrospun

Nanofibers Prepared from Poly((*N*-isopropylacrylamide)-*co*-(N-hydroxymethylacrylamide)) and Their Blends with 1,2-diaminoanthraquinone for NO Gas Detection. *Macromol. Chem. Phys.* **2014**, *215*, 286−294. [CrossRef]

37. Hung, C.C.; Kuo, C.C.; Weng, N.K.; Wu, W.C.; Chen, B.Y.; Cho, C.J.; Hsu, I.J.; Chiu, Y.C.; Chen, W.C. Novel Highly Sensitive and Reversible Electrospun Nanofibrous Chemosensor-Filters Composed of Poly (HEMA-*co*-MNA) and bpy-F-bpy with Metal-Ion-Modulated Multicolor Fluorescence Emission. *Polym. J.* **2016**, *48*, 439–449. [CrossRef]

38. Kim, Y.J.; Ebara, M.; Aoyagi, T. Temperature-Responsive Electrospun Nanofibers for 'On-Off' Switchable Release of Dextran. *Sci. Technol. Adv. Mater.* **2012**, *13*, 064203. [CrossRef]

39. Chuang, W.J.; Chiu, W.Y. Thermo-Responsive Nanofibers Prepared from Poly (N-isopropylacrylamide-co-*N*-methylol acrylamide). *Polymer* **2012**, *53*, 2829-2838. [CrossRef]

40. Chuang, W.J.; Chiu, W.Y.; Tai, H.J. Thermally Crosslinkable Poly(*N*-isopropylacrylamide) Copolymers: Synthesis and Characterization of Temperature-Responsive Hydrogel. *Mater. Chem. Phys.* **2012**, *134*, 1208-1213. [CrossRef]

Peer-reviewed version available at *Polymers* **2018**, *10*, 1259; doi:10.3390/polym10111259

Figure Captions

Figure 1. (a) SEM images of cross-linked **P1**, **P2**, and **P3** ES nanofibers in dry and wet states (treated with water). (b) Diameters of ES nanofibers at different temperatures.

Figure 2. PL spectra of ES fibers at different pH levels (pH 7–2): (a) **P2-Fibers**, (b) **P3-Fibers**. The insets show the detection of pH 2 and 12. PL spectra of ES nanofibers at a constant pH level (pH 2) and various temperatures (25–55 °C): (c) **P2-Fibers**, (d) **P3-Fibers** (λ_{ex}: 500 nm).

Figure 3. PL spectra obtained at various concentrations of Hg^{2+} (10^{-7}–10^{-3} M): (a) **P3-Fibers**, (b) **P3-film**, (c) comparison of relative PL intensity of ES nanofibers and thin film (λ_{ex}: 500 nm).

Figure 4. PL spectra of ES nanofibers at a constant Hg^{2+} concentration (10^{-3} M) and various temperatures (27–55 °C): (a) **P3-Fibers**, (b) relative trend graph of **P3-Fibers** (inset: photos of **P3** ES nanofiber membrane) (λ_{ex}: 500 nm).

Figure 5. (a) Fluorimetric response of **P3** ES nanofibers to various cations at 10^{-3} M in aqueous solutions of pH 7. From left to right: Hg^{2+}, Fe^{2+}, Pb^{2+}, Mg^{2+}, Zn^{2+}, Cu^{2+}, and K^{+} (black bar: immersed in aqueous solutions with Hg^{2+} or other metal ions; red bar: immersed in Hg^{2+} after sensing of other metal ions). (b) Hg^{2+}-dependent "on–off–on" fluorescence intensity profile of **P3** ES nanofibers (inset: photos of **P3** ES nanofiber membrane) (λ_{ex}: 500 nm).

Figure 6. (a) Confocal microscopy images of **P3** ES nanofibers at pH 2 and in aqueous solutions with Hg^{2+} ions (10^{-3} M; pH = 7.0). (b) Photos of the **P3** ES nanofiber membrane for sensing Hg^{2+} at pH 2 and various temperatures.

Figure 7. Schematic of a sensory fibrous membrane prepared using **P3**-based ES nanofibers,

which chelates and senses Hg^{2+} simultaneously.

Table 1. Molecular weights and thermal properties of poly(hydroxyethyl-*co*-NMA) and poly(NIPAAm-*co*-NMA-*co*-RhBN2AM) random copolymers.

Polymers	Feeding molar ratio NIPAAm:NMA:RhB	Experimental ratio[a] NIPAAm:NMA:RhB	Mn[b]	M_w/M_n[b]	Td[c] (℃)	LCST[d] (℃)
P1	**10:1:0.1**	**90.2:9.4:0.4**	**33 000**	**1.85**	**343**	**30.0**
P2	**10:3:0.1**	**80.5:19.2:0.3**	**35 300**	**1.92**	**351**	**35.0**
P3	**10:5:0.1**	**71.1:28.4:0.5**	**35 500**	**1.88**	**352**	**45.0**

[a] Molar ratio (%) estimated from ^{1}H NMR spectra.

[b] Determined by using a DMF eluent.

[c] Onset decomposition.

[b] Measured by using UV-Vis.

Preprints (www.preprints.org) | NOT PEER-REVIEWED | Posted: 22 October 2018 doi:10.20944/preprints201810.0478.v1

Peer-reviewed version available at Polymers 2018, 10, 1259; doi:10.3390/polym10111259

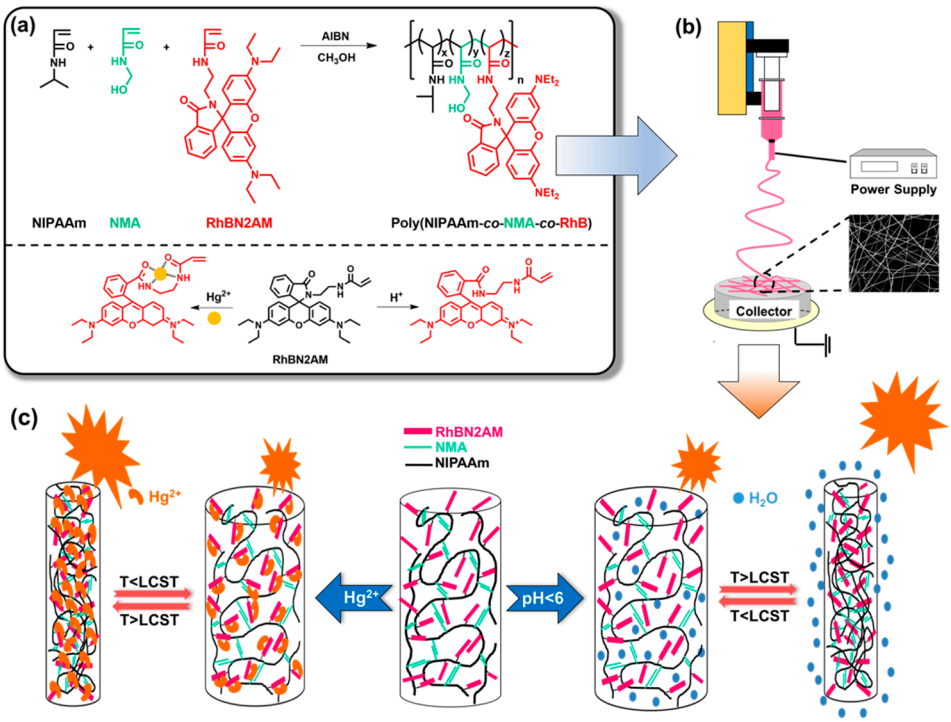

Scheme 1. Design of fluorescent ES nanofibers with multifunctional detection.

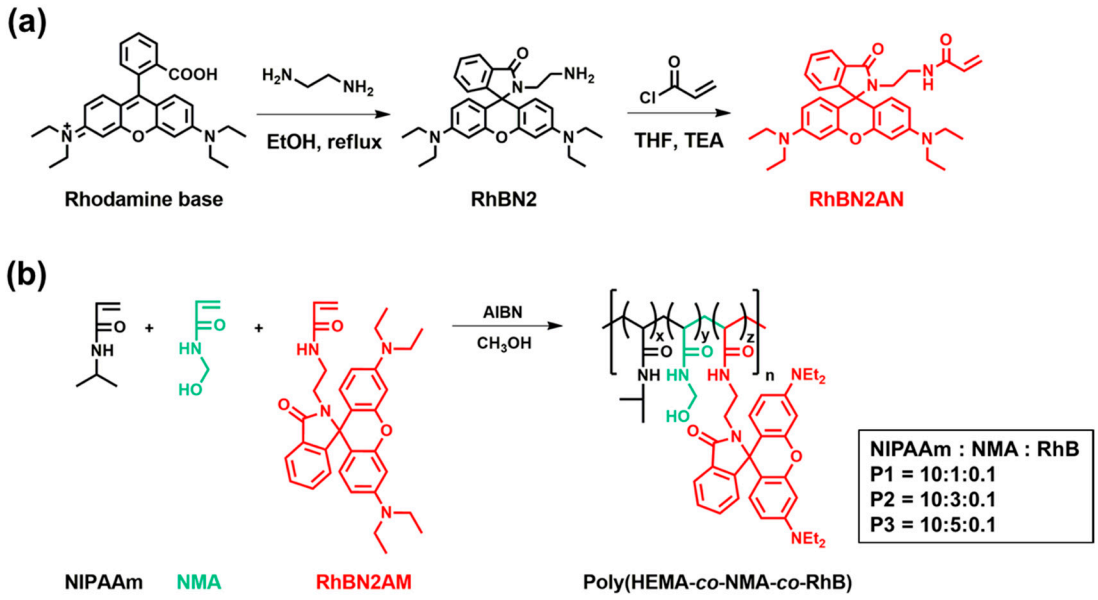

Scheme 2. Synthesis of (a) RhBN2AM (fluorescent probe), and (b) poly(NIPAM-*co*-NMA-*co*-RhBN2AM).

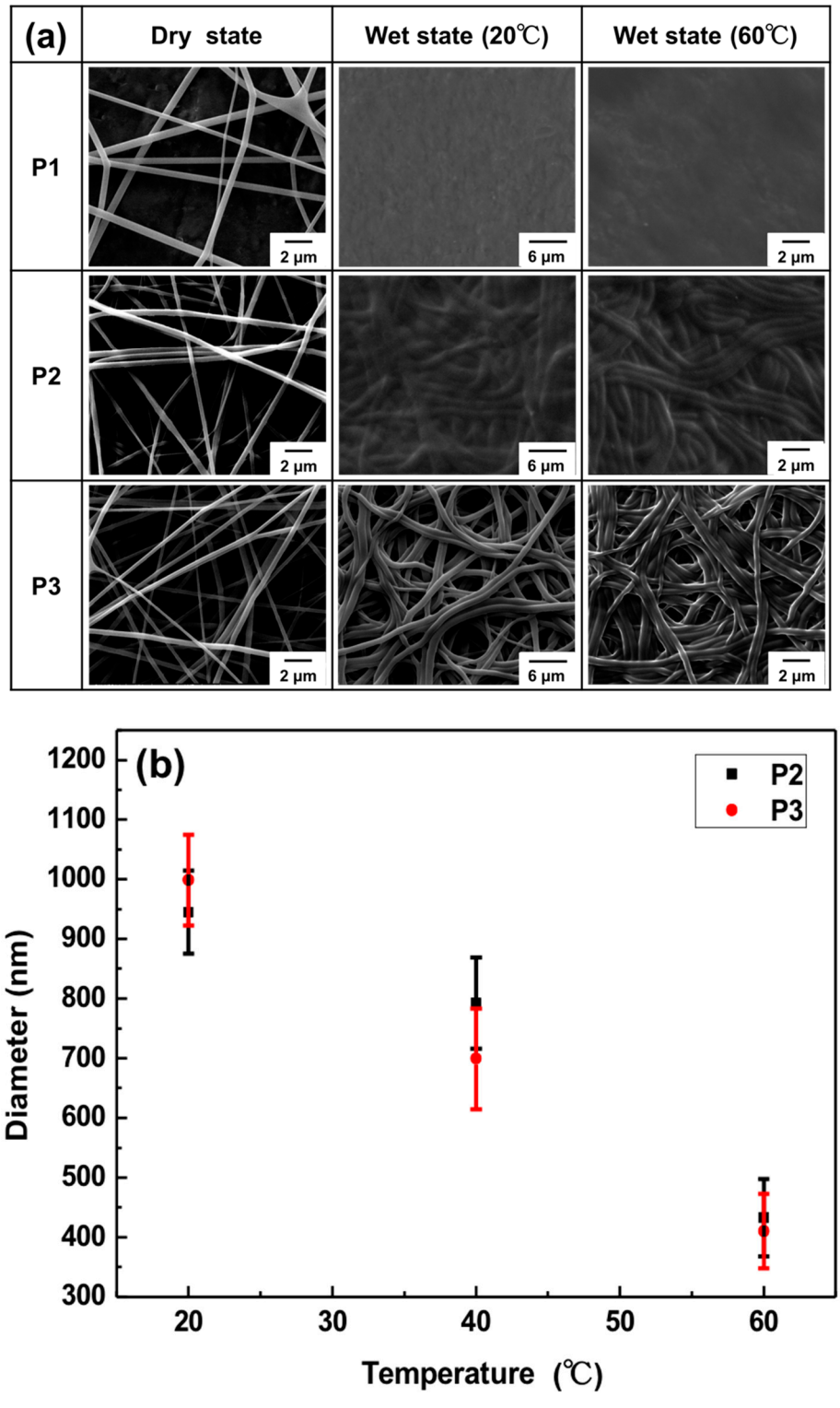

Figure 1

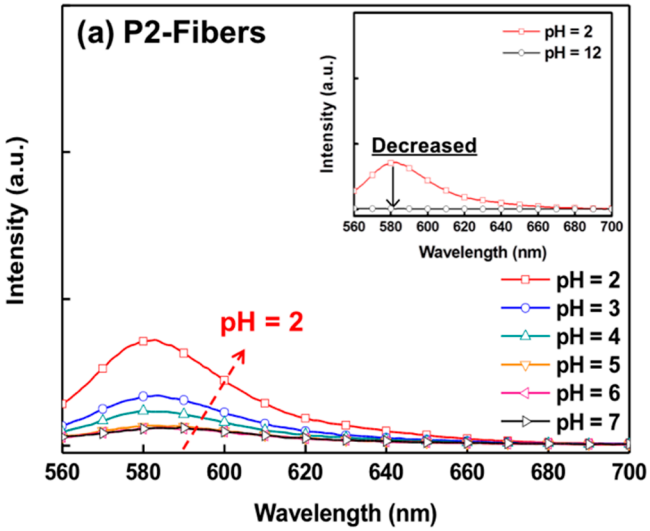

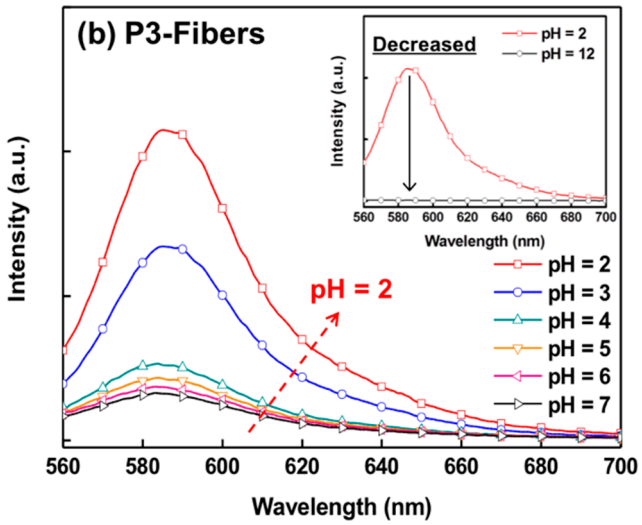

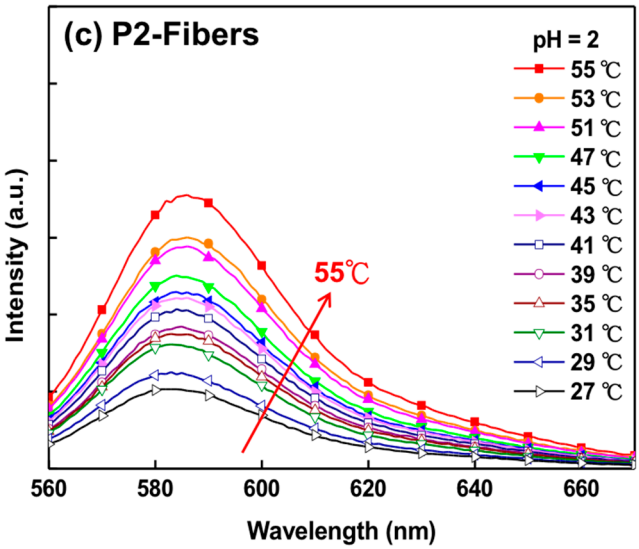

 doi:10.20944/preprints201810.0478.v1

Peer-reviewed version available at *Polymers* **2018**, *10*, 1259; doi:10.3390/polym10111259

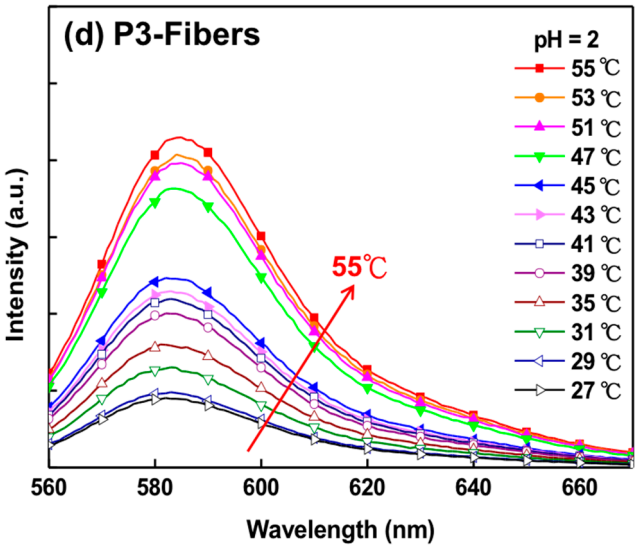

Figure 2

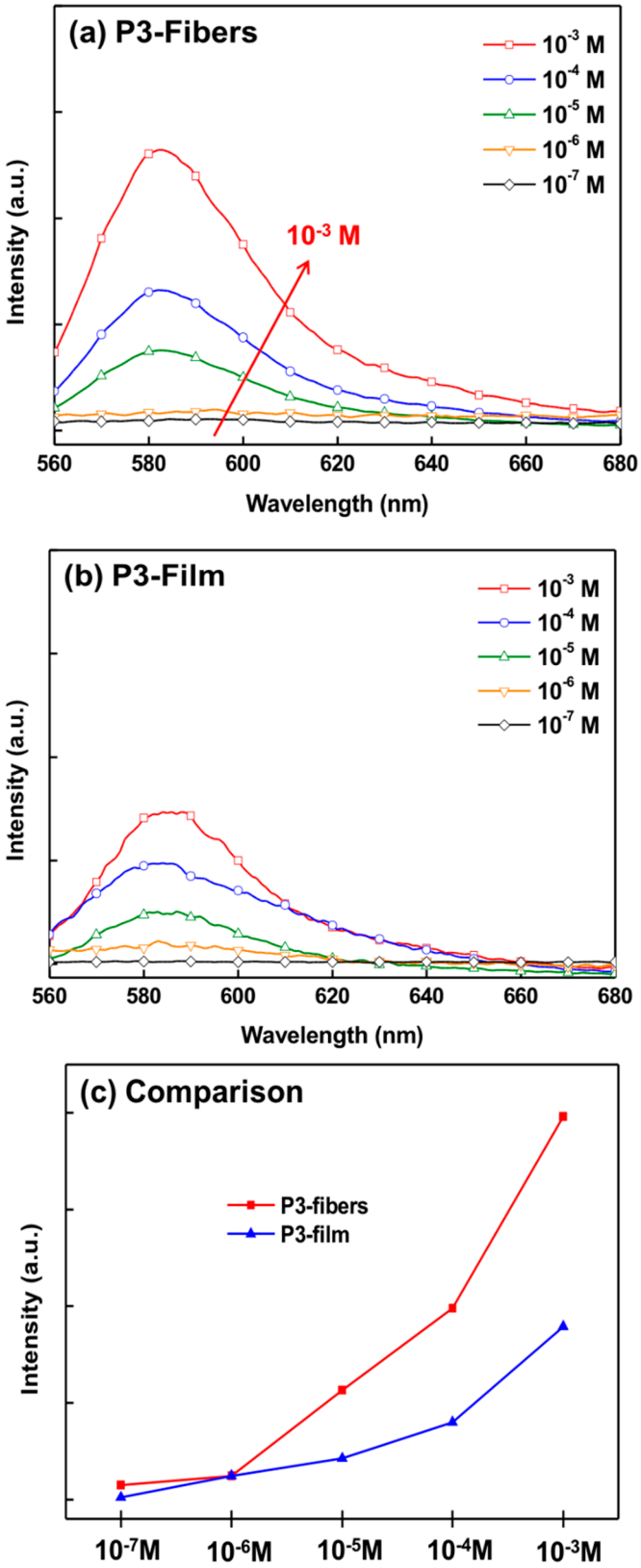

Figure 3

Preprints (www.preprints.org) | NOT PEER-REVIEWED | Posted: 22 October 2018 doi:10.20944/preprints201810.0478.v1

Peer-reviewed version available at Polymers 2018, 10, 1259; doi:10.3390/polym10111259

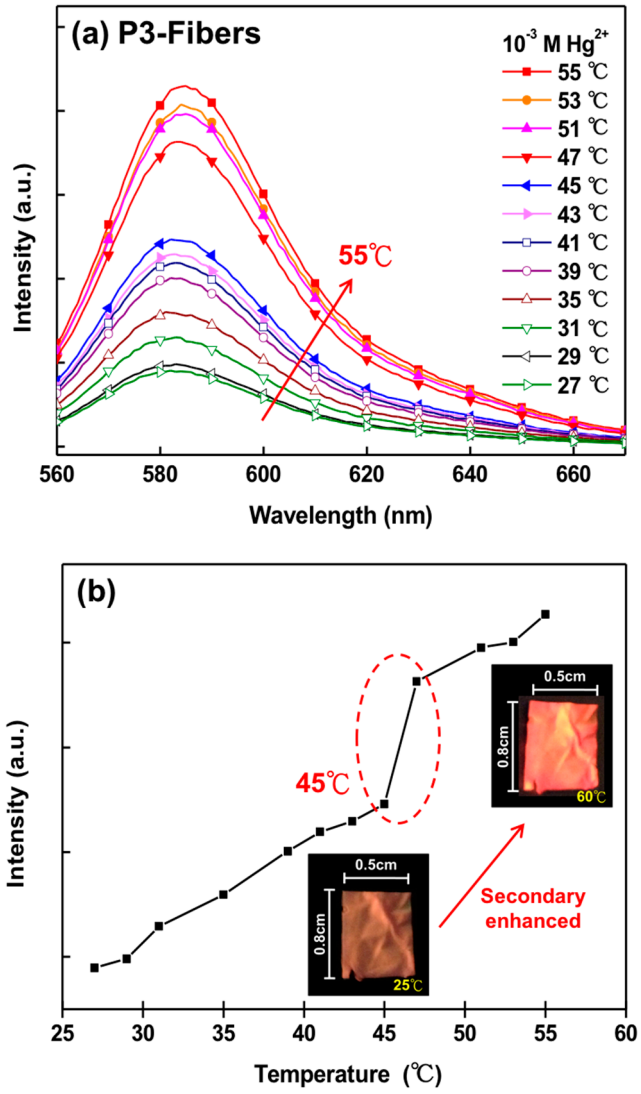

Figure 4

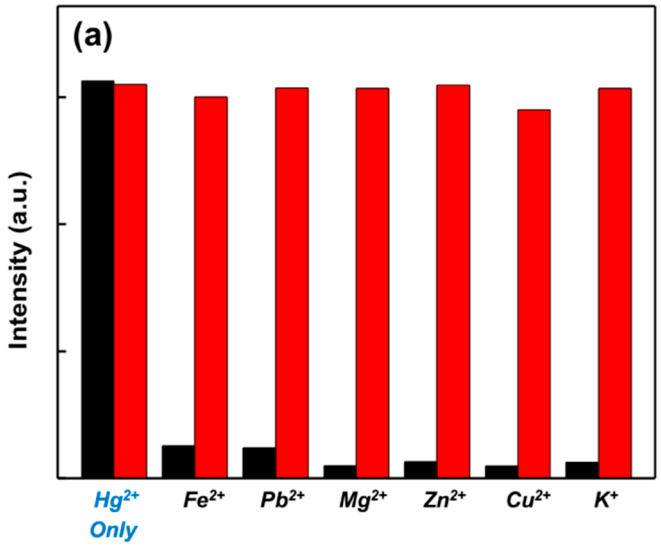

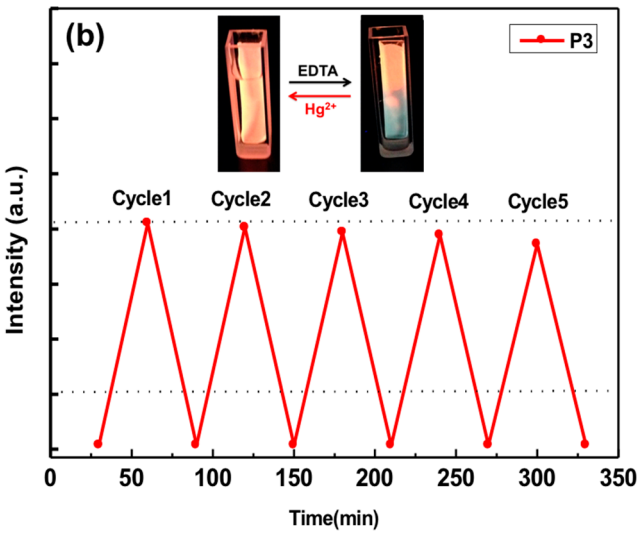

Figure 5

Preprints (www.preprints.org) | NOT PEER-REVIEWED | Posted: 22 October 2018 doi:10.20944/preprints201810.0478.v1

Peer-reviewed version available at Polymers 2018, 10, 1259; doi:10.3390/polym10111259

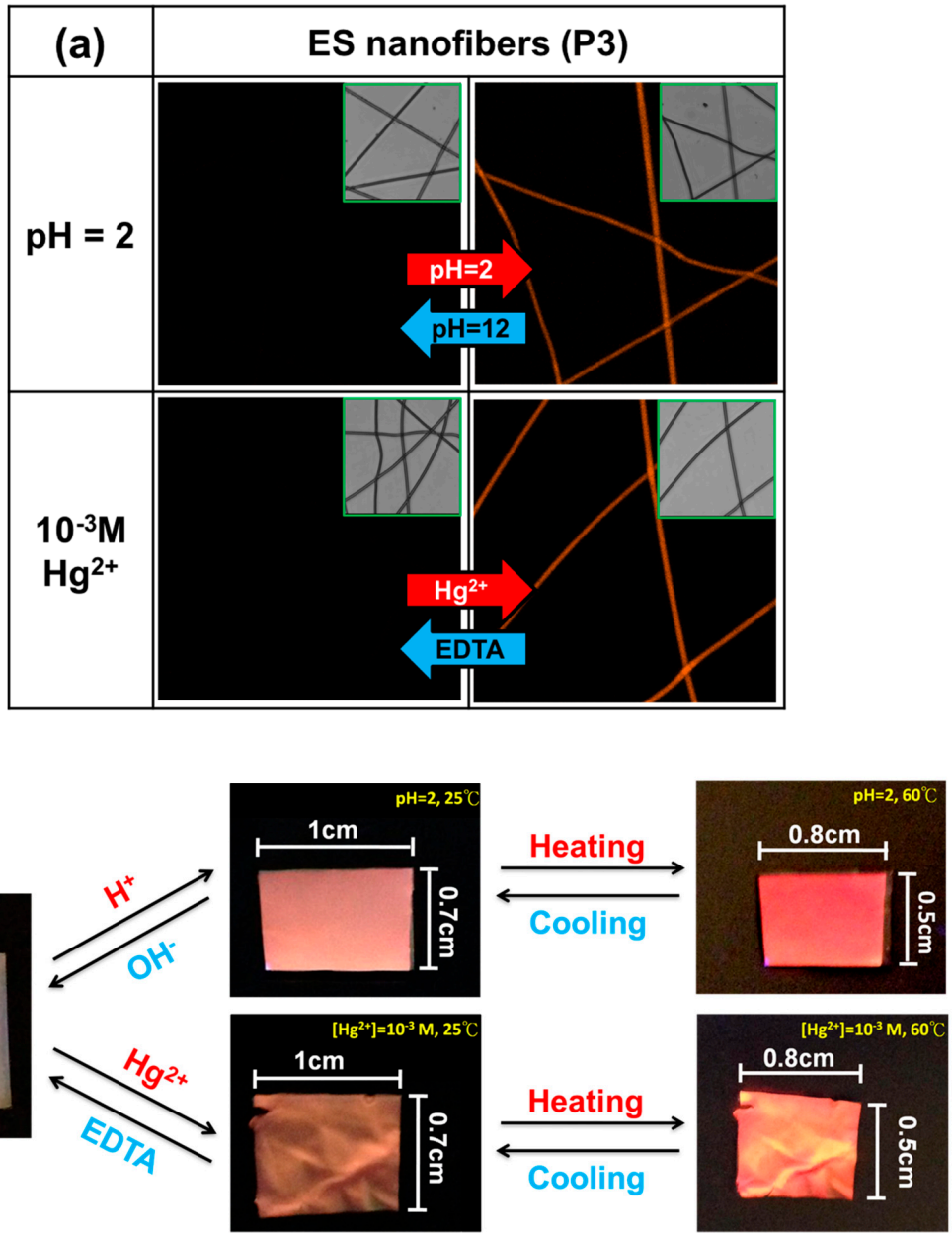

Figure 6

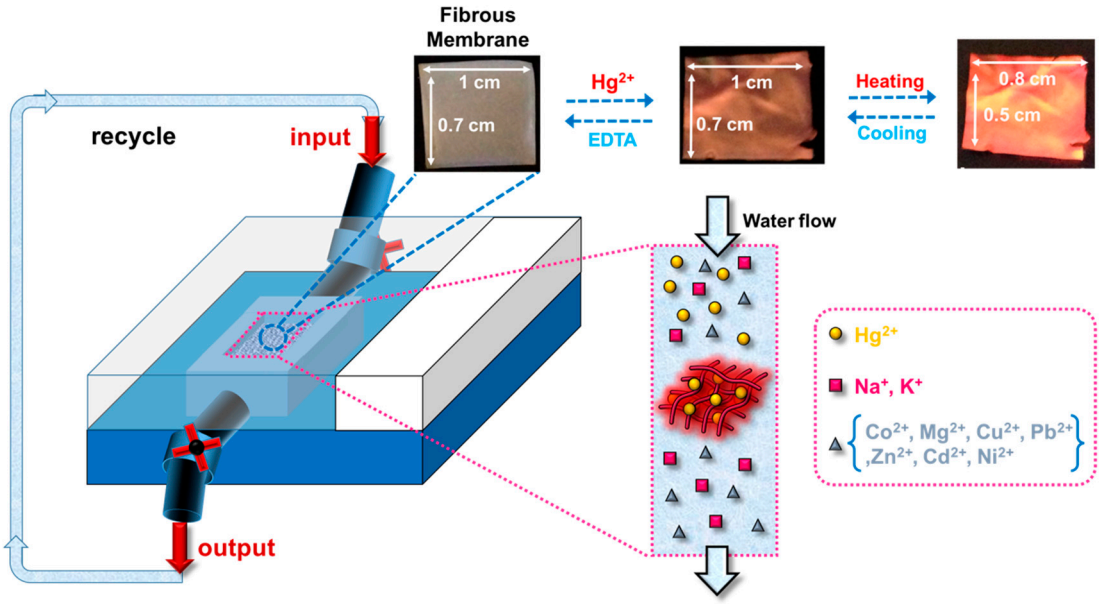

Figure 7

Peer-reviewed version available at Polymers 2018, 10, 1259; doi:10.3390/polym10111259

Supplementary Materials: Novel Multifunctional Luminescent Electrospun Fluorescent Nanofiber Chemosensors-filter and Their Versatile Sensing of pH, Temperature, and Metal Ions

Bo-Yu Chen [1,2,+], Yen-Chen Lung [2,+], Chi-Ching Kuo [2,3,*], Fang-Cheng Liang [2], Tien-Liang Tsai [2], Dai-Hua Jiang [2], Toshifumi Satoh [4], Ru-Jong Jeng [1,5,*]

Synthesis of the fluorescent probe (RhBN2) and fluorescent monomer (RhBN2AM)

The synthetic route was shown in Scheme 2(a). The synthesis of fluorescent probe, RhBN2, was performed according to a previous report [7]. Ethylenediamine (4.8 g, 10 mmol) were dissolved in 30 mL of ethanol. The mixture was immersed in an oil bath and refluxed for 20 h until the fluorescence of the solution disappeared. The solvent was removed under reduced pressure. CH_2Cl_2 (300 mL) was then added to the product, and the solution was washed with water several times and dried over an anhydrous magnesium sulfate. The filtrate was collected and solvent was removed under reduced pressure, to obtain pale-pink powder.

In a two-necked round-bottomed flask, RhBN2 (2 g, 4.14 mmol) was dissolved in 80 mL of THF, then TEA (2.88 mL) and excess acryloyl chloride were dropped into the stirred solution at 0 °C, the reaction mixture was stirred at room temperature for 1 day. The solution

Peer-reviewed version available at *Polymers* **2018**, *10*, 1259; doi:10.3390/polym10111259

was concentrated, then the resulting solid was purified by column chromatography using dichloromethane/methanol (20:1, v/v) as eluent. The chemical structure of RhBN2AM was characterized using ^{1}H NMR (**Figure S1(a)**) and ESI-MS (**Figure S1(b)**). ^{1}H NMR (300 MHz, $CDCl_3$, δ, ppm; **Figure S1(a)**): 6.24–7.88 (10H, Aromatic Hydrogen), 7.12 (1H, f), 6.15 (1H, g), 6.04 (1H, e), 5.55 (1H, e), 3.31 (10H, b, c), 3.13 (2H, d), 1.15 (12H, a). ESI-mass (**Figure S1(b)**): m/z calcd for $C_{33}H_{39}N_4O_3$+H^+([M+H^+]), found, 539.3010.

The Photoluminescence (PL) spectra based on ES Nanofiber for pH and Hg^{2+} sensing

Photoluminescence (PL) spectra were measured to study photophysical properties. PL experimental data were recorded using a Fluorolog-3 spectrofluorometer (Horiba Jobin Yvon). To ensure that the beam would excite the same point on the prepared samples at each measurement, the ES nanofibers were fixed in cuvettes by using an adhesive tape and the cuvette was filled with an aqueous metal ion solution at 10^{-7} to 10^{-3} M or acidic and basic aqueous solutions. Each measurement was maintained for 10 min to ensure that an equilibrium of the chelating reaction was reached. All PL spectra of the ES nanofibers were recorded using the Fluorolog-3 spectrofluorometer at an excitation wavelength of 540 nm, as described in our previous studies [28-37].

Preprints (www.preprints.org) | NOT PEER-REVIEWED | Posted: 22 October 2018 doi:10.20944/preprints201810.0478.v1

Peer-reviewed version available at Polymers 2018, 10, 1259; doi:10.3390/polym10111259

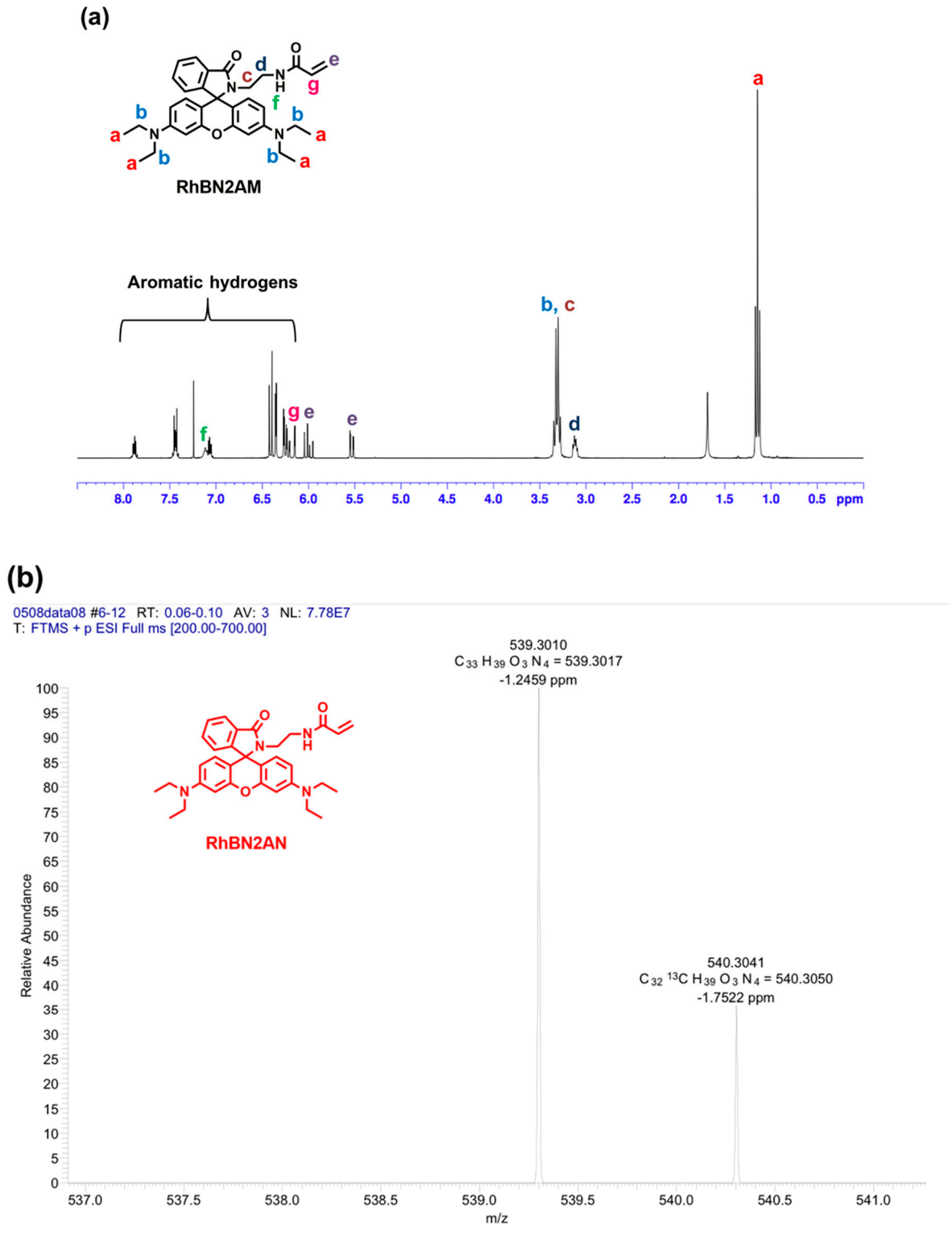

Figure S1. (a) ^{1}H NMR spectrum of RhBN2AM in $CDCl_3$. (b) ESI-MS spectrum of RhBN2AM.

Preprints (www.preprints.org) | NOT PEER-REVIEWED | Posted: 22 October 2018 doi:10.20944/preprints201810.0478.v1

Peer-reviewed version available at Polymers 2018, 10, 1259; doi:10.3390/polym10111259

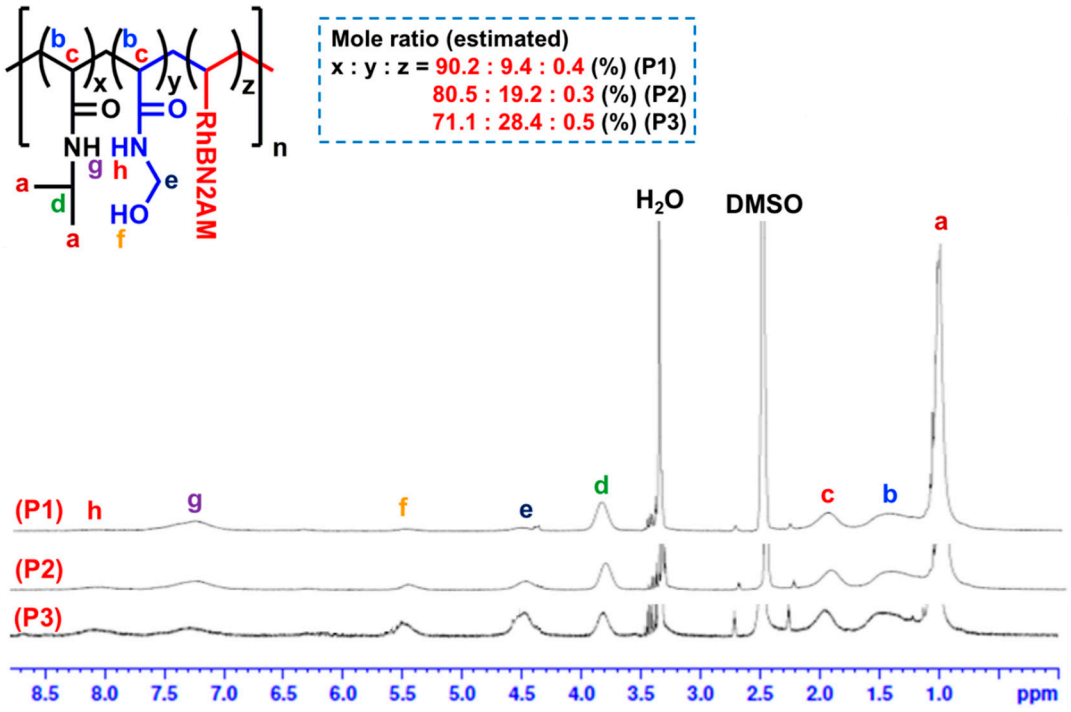

Figure S2. ^{1}H NMR spectra of **P1**, **P2,** and **P3.**

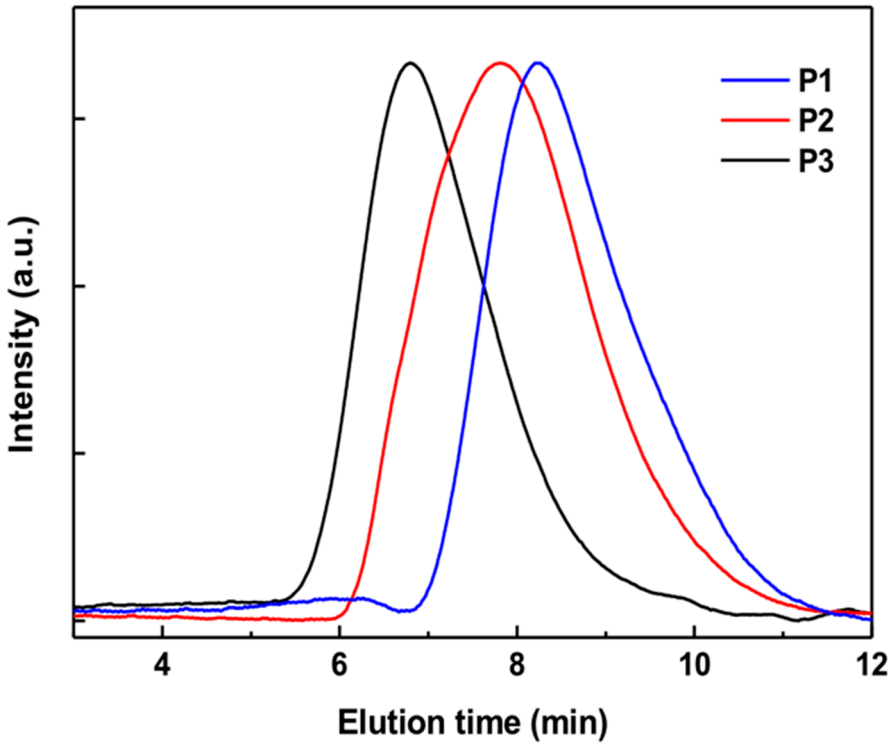

Figure S3. GPC profiles of **P1**, **P2**, and **P3**.

Preprints (www.preprints.org) | NOT PEER-REVIEWED | Posted: 22 October 2018 doi:10.20944/preprints201810.0478.v1

Peer-reviewed version available at Polymers 2018, 10, 1259; doi:10.3390/polym10111259

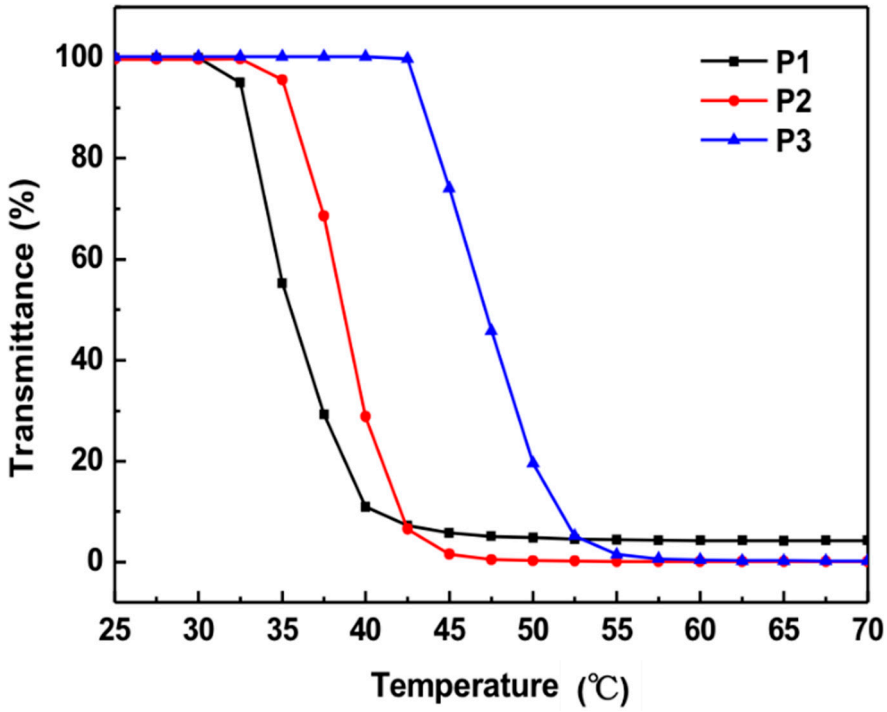

Figure S4. Variations in optical transmittance of **P1**, **P2**, and **P3** in water at temperatures from 25 to 70 °C.

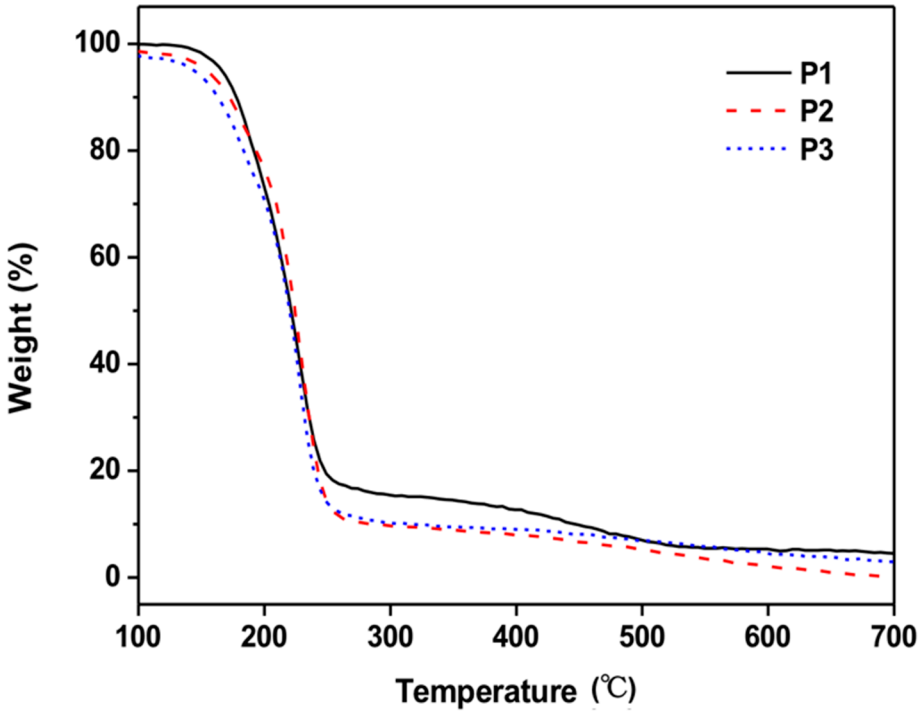

Figure S5. TGA curves of **P1**, **P2**, and **P3**.